Molecular Crystals and Liquid Crystals
Publication details, including instructions for authors and subscription information:
http://www.tandfonline.com/loi/gmcl20

Nematic Liquid Crystals and Nematic Colloids in Microfluidic Environment

A. Sengupta [a], S. Herminghaus [a] & Ch. Bahr [a]
[a] Max Planck Institute for Dynamics and Self-Organisation, Göttingen, Germany

Version of record first published: 16 Jun 2011

To cite this article: A. Sengupta, S. Herminghaus & Ch. Bahr (2011): Nematic Liquid Crystals and Nematic Colloids in Microfluidic Environment, Molecular Crystals and Liquid Crystals, 547:1, 203/[1893]-212/[1902]

To link to this article: http://dx.doi.org/10.1080/15421406.2011.572784

Mol. Cryst. Liq. Cryst., Vol. 547: pp. 203/[1893]–212/[1902], 2011

ISSN: 1542-1406 print/1563-5287 online
DOI: 10.1080/15421406.2011.572784

Taylor & Francis
Taylor & Francis Group

Nematic Liquid Crystals and Nematic Colloids in Microfluidic Environment

A. SENGUPTA, S. HERMINGHAUS, AND CH. BAHR

Max Planck Institute for Dynamics and Self-Organisation, Göttingen, Germany

We study nematic LCs and nematic colloids flowing through microchannels using polarizing transmission microscopy and fluorescence confocal polarizing microscopy. Depending on the channel dimensions, the anchoring conditions on the channel walls, and the flow rate, the formation of different textures and defect structures is observed: π-walls, disclination lines (DL) pinned to the channel walls, DL with one pinned and one freely floating end, and DL and loops freely floating in a chaotic-like manner. Preliminary observations of nematic LCs containing colloidal particles indicate that textures and defects of the nematic matrix can be used to guide the transport of the particles through the microchannels.

Keywords colloid transport; colloid trapping; flow-induced textures and defects; flow-stabilized defects; microfluidics; π-walls

1. Introduction

Novel colloidal systems consisting of colloidal particles dispersed in nematic liquid crystals (NLCs) have recently attracted large interest [1–3]. In these systems, the colloidal pair interaction is not of the van der Waals or electrostatic type, but stems from the elasticity of the director field of the nematic host. A direct manipulation of these systems can be achieved by means of optical tweezers. A different manipulation approach could be the use of forces which are present when the systems flow through an appropriate microfluidic device. Nematic colloids flowing through microchannels have not been studied so far. Even pure NLCs (not containing colloidal particles) have been rarely studied in microfluidic environment [4].

In this paper, we report on optical polarizing microscopy and confocal fluorescence microscopy studies of NLCs and nematic colloids flowing through microchannels. Using microfluidics, we are able to confine NLCs to microscale dimensions and create well defined flow situations. Different kinds of texture and defect structures in flowing NLCs are generated depending upon channel dimensions, flow velocities and anchoring conditions on the walls of the microchannels. The obtained structures can be manipulated using the flow field within the channel, e.g., by varying the mean flow velocity within the channel. Various regimes in the parameter space of flow

Address correspondence to A. Sengupta, Max Planck Institute for Dynamics and Self-Organisation, Am Fassberg 17, D-37077 Göttingen, Germany. Tel.: +49 551 5176 214; Fax: +49 551 5176 202; E-mail: anupam.sengupta@ds.mpg.de

velocity and channel depth are obtained within which the different structures are stable. We report also preliminary observations on the behavior of colloidal particles in NLCs flowing through microchannels.

2. Experimental Methods

Microchannels were constructed by plasma gluing polydimethylsiloxane (PDMS) reliefs, prepared by soft lithography, on glass substrates. For the initial studies described here, we prepared simple linear channels with a rectangular cross section; their height h was varied between 5 and 100 μm and their width w was chosen from 50 to 100 μm. The distance between the inlet and the outlet ports was 2.5 mm, defining the length of the channels. The length of the channels was much longer than the two other dimensions in order to ensure that the observations recorded were in the fully developed flow regime. Throughout this article, we would refer to the plan view of the microchannels as XY plane. Consequently YZ plane would refer to the plane to which the flow is perpendicular. Figure 1 shows the relevant coordinate system in consideration. Two teflon tubes having inner and outer diameters of 300 μm and 760 μm respectively, which were inserted into soft PDMS body, one each at the inlet and outlet ports, served as connectors between inlet-source and outlet-sink respectively. The inlet tube was connected to an air-tight microlitre syringe, driven by a gear pump with sub-microlitre precision.

The syringe pump was filled with the common NLC compound 5CB (Synthon Chemicals, used as received). The flowing NLC in the channel was directly observed using optical polarizing transmission microscopy (PM). Static textures and structures remaining after a stop of the flow were subsequently studied using flourescence confocal polarizing microscopy (FCPM) [5]; for this purpose, the 5CB was doped with a small amount of the dye Nile Red (concentration ~0.01%) which aligns along the director of the NLC.

The anchoring on the PDMS walls of the microchannels is near homeotropic under normal conditions. However, after plasma treatment, the anchoring changes from homeotropic to degenerate planar [6] as is manifested by the non-zero birefringence, easily detected with crossed polarizers, of the NLC on such a PDMS substrate. The plasma-treated glass surface constructing the bottom of the channel has also a degenerate planar anchoring. For some studies, we used instead of the

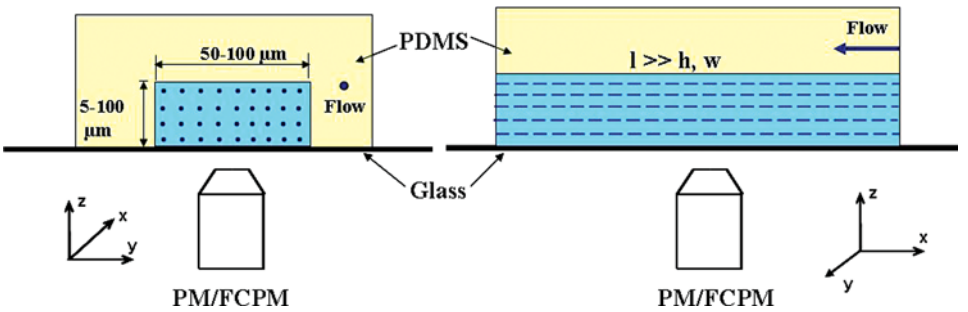

Figure 1. Experimental set up: the flow of the NLC through a microfluidic channel is studied by PM and FCPM; left: channel cross section perpendicular to flow direction, right: cross section parallel to flow. (Figure appears in color online.)

plasma-treated type, a glass coated with an aligning layer inducing a uniform planar anchoring.

The volume flow rate within the microchannels was varied from 2 to 40 microliters per hour. Under the given channel dimension and flow conditions, the mean velocity of the NLC in the microchannels varied between 1 to 22 mm/s, with the Reynolds number ***Re*** lying between 10^{-4} to 4.5×10^{-3}. With respect to hydrodynamics, this ensured a strictly laminar flow.

3. Results and Discussion

Most experiments were conducted with microchannels in which all four walls possessed a degenerate planar anchoring. The corresponding results are described in the following section. Experiments concerning the transport of colloidal particles (Section 3.2) were conducted in channels prepared with glass plates which were coated with a rubbed polymer layer; thus, these channels possessed one uniform planar anchoring (glass) and three degenerate planar anchoring (PDMS) walls.

3.1. *Texture Development in Degenerate Planar Anchoring Channels*

3.1.1. *Spontaneous Formation of π-walls.* With small channel depths $<10\,\mu m$, and low (~ 0 mm/s) to intermediate (~ 15 mm/s) mean flow rates, the spontaneous creation of π-walls are observed. Under crossed polarizers, they appear as alternate dark and bright stripes. Figure 2 shows such a set of π-walls.

The π-walls are created by the impact of flow on ± 1 disclination lines extending from the top to the bottom of the channel. These disclination lines, which are also responsible for the typical appearance of the static schlieren texture in thin nematic films, form spontaneously when the channel is filled and move downstream along with the flowing NLC. By this process, the four brushes which originate from a ± 1 disclination (and which extend in four different directions in a static schlieren texture) are aligned along the flow direction and form a set of parallel π-walls extending up to several hundred μm in length. They are stable not only under flow situations, but also long time ($\sim 24-36$ hours) after the flow has ceased. The π-walls formed in this way show a uniform wavelength under a particular flow rate (Fig. 3), gradually giving way to non-uniform wavelengths and other defect structures once the mean flow velocity is increased.

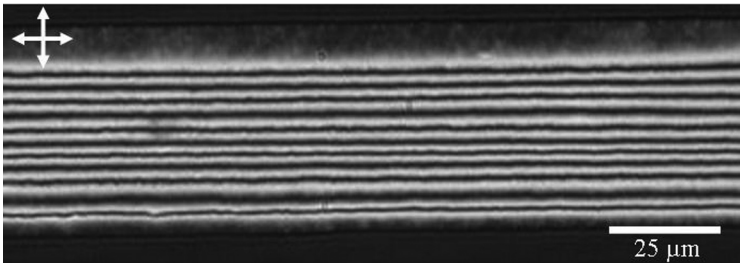

Figure 2. Set of π-walls in a 8 μm (h) × 100 μm (w) channel obtained at a flow rate of 20 μl/h. Arrows indicate the orientation of crossed polarizers.

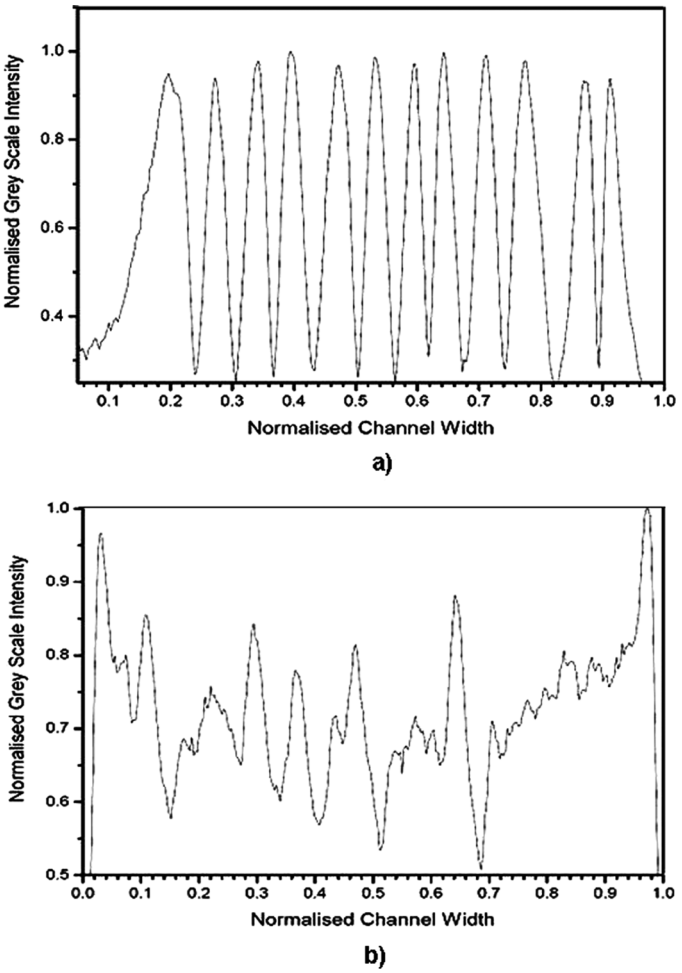

Figure 3. Wavelength of π-walls in a $8\,\mu m \times 100\,\mu m$ channel obtained at a flow rate of (a) $20\,\mu l/h$ and (b) $27.5\,\mu l/h$.

To study the director profiling of the π-walls in space, FCPM studies were conducted with 5CB samples containing 0.01% of the dye Nile Red which aligns with its transition dipole moment along the nematic director. High fluorescence intensities are then obtained for those regions of the sample in which the director is parallel to the polarization of the exciting laser light. Fluorescence intensities were captured in the XY plane at various depth values Z so that in-plane images and cross sections can be obtained. Figure 4 shows FCPM images in two different planes of one such set of π-walls.

Combining the PM and FCPM imaging, the director profile of the π-walls is obtained as one shown in Figure 4c. The FCPM image of a π-wall cross section shows that the π-walls stack up in Z direction. When viewed under white light, the π-walls are invisible. The leading edge of the π-wall set, which is typically a ± 1 disclination, is however visible under white light as a small black dot. This confirms that the π-walls stack one plane over another, from the bottom to the top of

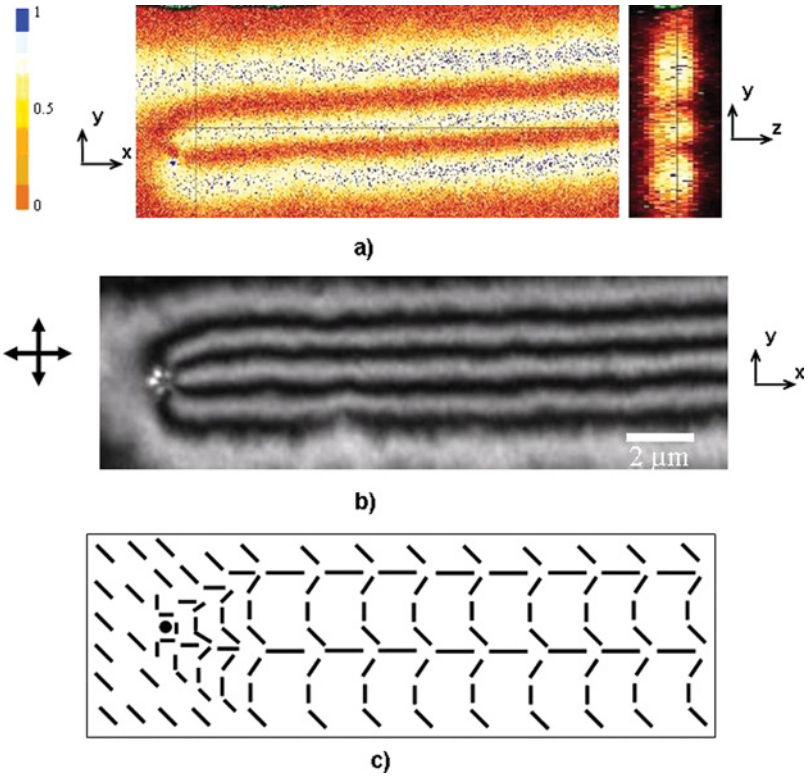

Figure 4. (a) FCPM image of π-walls along XY and YZ planes; the exciting light was polarized parallel to the channel, in the high intensity regions (white and blue colour) the nematic director is parallel to the polarization direction. (b) Micrograph of the same π-wall set obtained with crossed polarizers; the π-walls originate from the ± 1 disclination (at the left edge) which moves with the flow through the channel. (c) Director profile of the π-walls. (Figure appears in color online.)

the channel, without the director coming out of the XY plane. The stacks are held together by the disclination line at the leading edge of the π-wall structure, which extends from the bottom to the top of the channel.

3.1.2. *Termination of π-walls at Surface-Stabilized Disclinations.* On increasing the mean flow velocities ($\sim$18 mm/s) within the channel, the disclination line extending from the bottom to the top of the channel in the π-wall gets unpinned from the lower surface and aligns itself horizontally in the flow direction. This can also be observed at relatively lower flow rates, however with deeper channels, $10\,\mu\text{m} < h < 20\,\mu\text{m}$. The horizontal disclinations originate at the leading edge of the π-walls and extend longitudinally along the channel length, in the flow direction (Fig. 5). The terminating end of the disclination is also pinned on the same surface of the channel, either extending linearly from the π-walls, or forming a curved open loop in the downstream direction. In the following, we designate these disclinations as "surface-stabilized" disclination lines. Surface-stabilized disclinations are very stable both under a given flow rate or in absence of any flow after their formation. As shown in Figure 5b, they are clearly visible under

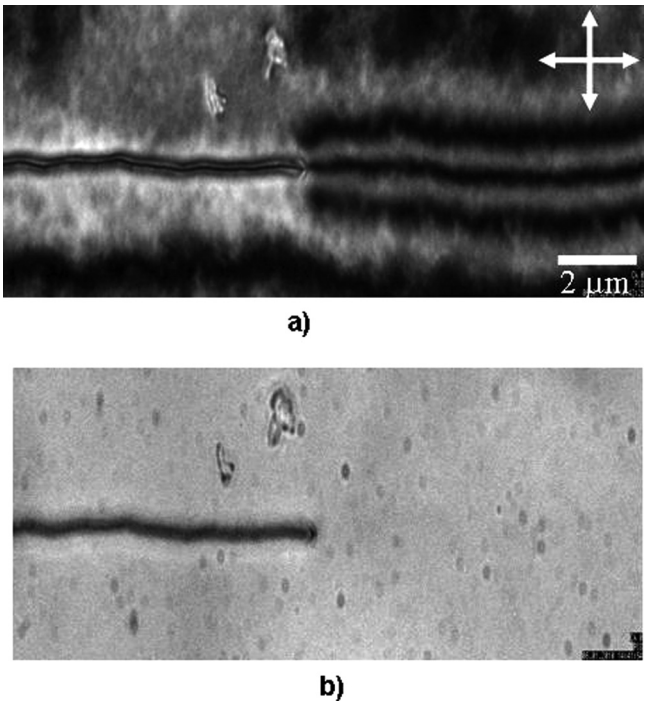

Figure 5. Surface-stabilized disclination line with origin at π-wall, viewed under (**a**) crossed polarizers and (**b**) white light.

white light whereas the terminating π-wall structure is observed only under crossed polarizers.

3.1.3. *Flow-Stabilized Disclinations.* On increasing the mean flow velocity further ($>$18 mm/s), the surface-stabilized disclinations give way to the third kind of flow induced defect structure, the flow-stabilized disclinations. These defects are disclination lines which are pinned only at one end. The other end of the disclination exists downstream of the channel, stretched freely in the bulk of the NLC flowing through the microchannel. The length of such disclination lines, defined as the distance of the free end of the disclination from the point of pinning, is strongly dependent on the mean velocity of the flow and it shrinks to zero when the flow is stopped. We therefore designate these disclinations as ''flow-stabilized'' disclinations. The flow-stabilized disclinations are visible under crossed polarizers and under white light due to the scattering of light by them.

If the velocity of the flow is increased above a certain value ($>$20 mm/s), the free end of the disclination starts oscillating about a mean point. On increasing the flow rate further, the amplitude of the oscillations increases (Fig. 6). This is accompanied by the increment of the length of the disclination itself. This dual increment of the length of the disclination and the amplitude of the oscillations continues till a certain critical value of flow rate, beyond which the system enters a chaotic-like regime in which disclinations are freely flowing. Before reaching the

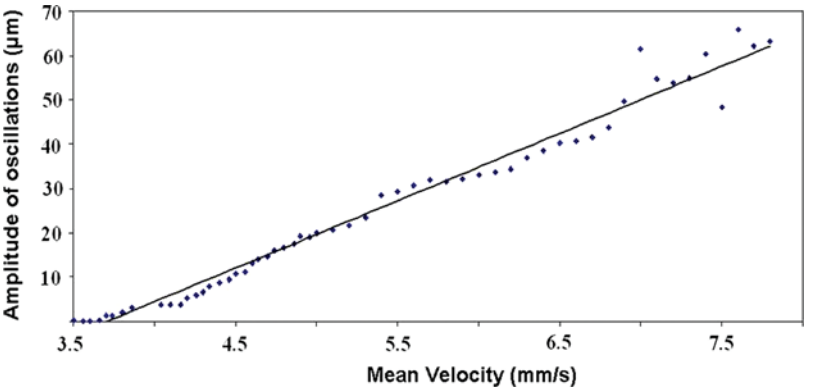

Figure 6. Dependence of the amplitude of the oscillations of flow-stabilized disclination lines on the mean flow velocity. (Figure appears in color online.)

critical value, if the flow rate is reduced, so do the length of the disclination and the oscillation amplitude.

The critical value of flow rate reduces with the increase in the depth of the channel. For deeper channels, the entrance to the chaotic regime takes place at lower flow velocities. Beyond a channel of depth of ~25 μm, the textures directly enter the chaotic regime, even at low values of the mean velocity. The chaotic regime is characterized by numerous freely flowing disclinations, both straight lines and loops. These defects vigorously interact with each other, intertwining, annihilating and crossing each other. Figure 7 shows in which regions of the channel depth vs. flow velocity parameter plane the various defect structures are stable.

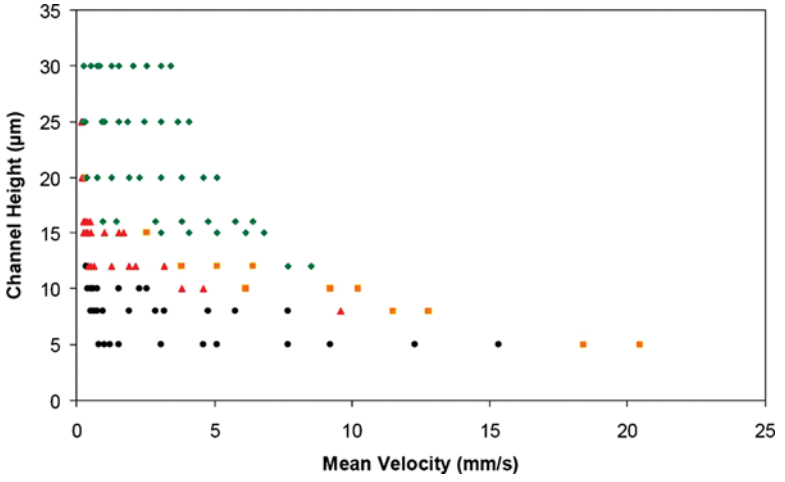

Figure 7. Observed defect structures in the mean flow velocity vs. channel height parameter plane (w = 50 μm). Black dots: π-walls, red triangles: surface-stabilized disclinations, yellow squares: flow-stabilized disclinations, green rhombus: chaotic-like regime with freely floating disclinations. (Figure appears in color online.)

3.2. *Behaviour of Colloid Particles in the Flow Field*

Colloid particles possessing homeotropic anchoring conditions on their surface exhibit two different kinds of topological defects when introduced in a uniform director field: they are accompanied either by a topological point defect (“hyperbolic hedgehog”) or by a circular disclination line (“saturn ring”). The deformation of the director field leads to long range interactions, analogous to either dipolar (hedgehog) or quadrupolar (saturn ring) electric interactions, between the particles [1,2]. Similar interactions are present between the particles and defect structures such as disclination lines [7]. We report here preliminary observations concerning the behavior of such particles in NLCs flowing through microchannels.

The colloids used for the present study were spherical polystyrene beads (Licristar), having a mean diameter of ~4.5 μm, treated with 0.5% aqueous DMOAP solution. For the preparation of the microchannels, we used glass plates which were coated with a rubbed polyvinyl alcohol layer. Thus, the channels possessed three walls with degenerate planar anchoring (PDMS) and one wall with uniform planar anchoring (coated and rubbed glass). If the rubbing direction is parallel to flow direction, a homogeneous director field is obtained at low flow rates. Under these conditions, the colloidal particles (either single particles or linear assemblies) are transported through the channel in a selectively oriented configuration as is shown schematically in Figure 8.

If we prepare the microchannels such that the rubbing direction on the glass wall is perpendicular to the flow direction, we observe the frequent generation of disclination lines, aligning parallel to the flow direction and pinned at both ends to the channel walls. If colloidal particles are transported through such channels, they are trapped by the disclination lines and follow then exactly the course of the disclination line (Fig. 9). If the particles reach the pinned end of the disclination line, they get separated from the line provided the force on the particles which is

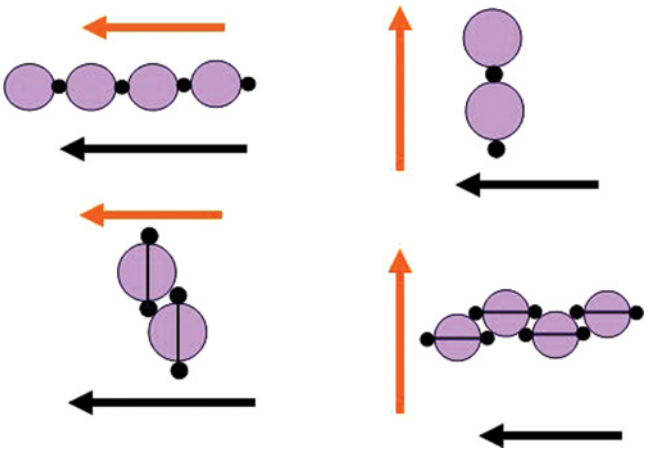

Figure 8. Selectively oriented transport of colloidal particles in a flowing NLC possessing a homogeneous director field; black arrows: flow direction, orange arrows: rubbing direction on the channel wall. Top: particles with hedgehog defect, bottom: particles with saturn ring. (Figure appears in color online.)

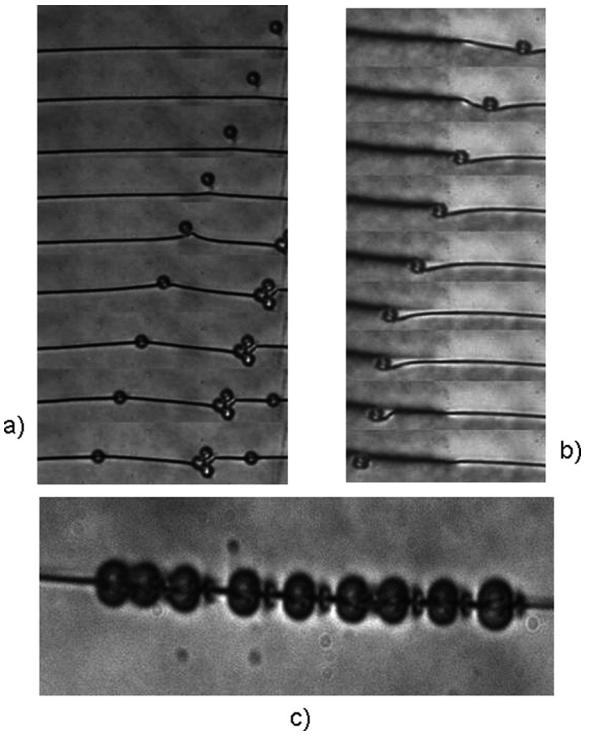

Figure 9. Transport of 5 μm colloidal particles by disclination lines in a microchannel: a) Capture of a colloidal particle by a disclination line and subsequent transport. b) Separation of a colloidal particle from a disclination line. Time proceeds from top to bottom, time difference ~0.33 s between consecutive images. c) Linear colloidal rail of particles transported through a disclination line.

generated by the flowing NLC matrix is large enough to overcome the interaction between the particles and the disclination line.

4. Conclusions and Perspectives

We have studied the flow of the NLC 5CB through microchannels possessing a rectangular cross section and three PDMS and one glass wall. Depending upon the channel dimensions and flow velocities, different kinds of structures are created. In shallow channels ($w = 50\,\mu m$, $h = 10\,\mu m$), we observe with increasing flow velocity the formation of π-walls, disclination lines pinned to the channel walls, disclination lines with one freely floating end, and disclination lines and loops flowing freely in a chaotic-like manner. The same sequence of structures is observed if we increase the channel depth at constant flow velocity. The structures extend to long length scales, often a few hundred micrometers. They influence the transport of colloidal particles suspended in the NLC matrix: the local director field determines the orientation of single particles and linear particle assemblies during the transport and disclination lines can trap the particles and guide their transport. Future studies in this field may provide a potential means of attaining colloid assemblies in complex geometries.

Acknowledgment

This research was supported by the European Union (Marie Curie Initial Training Network "Hierarchical Assembly in Controllable Matrices, HIERARCHY"), grant no. 215851. Helpful discussions with I. Musevic and A. Nych as well as the hospitality during a stay at the J. Stefan Institute in Ljubljana are gratefully acknowledged.

References

[1] Poulin, P., Stark, H., Lubensky, T. C., & Weitz, D. A. (1997). *Science*, *275*, 1770.
[2] Musevic, I., Skarabot, M., Tkalec, U., Ravnik, M., & Zumer, S. (2006). *Science*, *313*, 954.
[3] Musevic, I., & Skarabot, M. (2008). *Soft Matter*, *4*, 195.
[4] Jewell, S. A., Cornford, S. L., Yang, F., Cann, P. S., & Sambles, J. R. (2009). *Phys. Rev.*, *E80*, 041706.
[5] Smalyukh, I. I., Shiyanovskii, S. V., & Lavrentovich, O. D. (2001). *Chem. Phys. Lett.*, 336.
[6] Shojaei-Zadeh, S., & Anna, S. L. (2006). *Langmuir*, *22*, 9986.
[7] Pires, D., Fleury, J. B., & Galerne, Y. (2007). *Phys. Rev. Lett.*, *98*, 247801.